INSTITUT D'AERONOMIE SPATIALE DE BELGIQUE

3, avenue Circulaire, UCCLE - BRUXELLES 18

AERONOMICA ACTA

A - N° 13 - 1961

Density of the heterosphere related to temperature

by M. NICOLET

BELGISCH INSTITUUT VOOR RUIMTE-AERONOMIE

3, Ringlaan, UKKEL - BRUSSEL 18

SAO Special Report No. 75

DENSITY OF THE HETEROSPHERE RELATED TO TEMPERATURE

by

Marcel Nicolet

Smithsonian Institution
Astrophysical Observatory

Cambridge 38, Massachusetts

DENSITY OF THE HETEROSPHERE RELATED TO TEMPERATURE

by

Marcel Nicolet[1]

Summary. --Atmospheric models based on diffusion equilibrium in which helium plays a role are derived by use of heat conduction as the essential process that determines the gradient of temperature.

Introduction of boundary conditions at 120 km, where diffusion begins for major constituents, leads to atmospheric models that can be used for analysis of variations of day-to-night and solar activity in the whole thermosphere from 150 km to 2000 km.

Physical parameters such as density, pressure, concentration, mean molecular mass and local scale-height are given as functions of the temperature, which is considered the fundamental parameter.

An analysis of the behavior of the heterosphere, i.e., of the terrestrial atmosphere where the mean molecular mass cannot be taken as a constant parameter, requires a theoretical study to supplement observational results from which it is not yet possible to obtain all the parameters needed for a complete picture of the physical conditions.

If a general consistent picture of the vertical distribution of density in the heterosphere at heights between 200 km and 1500 km is obtained from acceleration data derived from earth-satellite orbits, the analysis leads sometimes to unjustified conclusions concerning the physical conditions. The sharp increase of molecular mass, the gradient of temperature increasing with height, the inflection of density curves, and the correlation of density with unusual indices of solar activity are among other physical anomalies that are introduced into this analysis.

---

[1]Consultant, Smithsonian Astrophysical Observatory, Cambridge, Mass.

In this paper, an improved method for calculating physical parameters of the heterosphere is applied, in which the temperature is selected as the essential parameter, and diffusion and heat conduction are introduced.

1. Formulas for Density

The vertical distribution of the upper atmosphere density deduced from the rate of change of the period of the motion of a satellite in its orbit is generally represented by the formula

$$\rho = \rho_0 \exp(-z/H_\rho) \quad , \tag{1}$$

in which ρ denotes density at height z, and ρ_0 at $z = 0$; and H_ρ is a parameter of the vertical distribution of density, which must be defined by

$$\frac{1}{\rho}\frac{d\rho}{dz} = -\frac{1}{H_\rho} \quad , \tag{2}$$

with the condition

$$dH_\rho/dz = 0. \tag{3}$$

These formulas cannot lead to correct conclusions concerning the temperature or the mean molecular mass in the heterosphere.

To provide a basis for an analysis of the vertical distribution of the temperature and mean molecular mass, we must use at least the general formula representing conditions of a perfect gas and of hydrostatic distribution.

The general form to be used is (Nicolet, 1954)

$$\frac{dp}{p} = \frac{dn}{n} + \frac{dT}{T} = -\frac{dz}{H} \quad , \tag{4}$$

where p is the total pressure; n is the total molecular concentration; T is the absolute temperature; and H is the local atmospheric scale-height. The atmospheric scale-height H is defined by

$$H \equiv \frac{kT}{mg} \quad , \tag{5}$$

where m is the mean molecular mass; g is the acceleration of gravity; and k is Boltzmann's constant. The variation is, therefore, related to the variation of T, m and g; that is,

$$\frac{dH}{H} = \frac{dT}{T} - \frac{dm}{m} - \frac{dg}{g} \quad . \tag{6}$$

By using equation (6), and introducing the gradient of the atmospheric scale height

$$\beta \equiv dH/dz \ , \tag{7}$$

we find that the general equation (4) leads to

$$\frac{1}{p}\frac{dp}{dz} = -\frac{1}{H} \ , \tag{8}$$

and

$$\frac{1}{\rho}\frac{d\rho}{dz} = -\frac{1+\beta}{H} \ . \tag{9}$$

Thus, from equations (2) and (9), the relation between the local atmospheric scale height H and the density parameter H_ρ is

$$H = (1+\beta)\ H_\rho \ . \tag{10}$$

The values of H_ρ, which are deduced from the slope of the density-versus-altitude curve, cannot represent real atmospheric conditions. The use of H_ρ may lead to wrong conclusions about the structure of the thermosphere, especially where the gradient of the atmospheric scale height is large.

If the height interval is small enough, β can be assumed constant for calculation purposes. If equations (8) and (9) are written in the form

$$\frac{dp}{p} = -\frac{1}{\beta}\frac{dH}{H} \ , \tag{11}$$

and

$$\frac{d\rho g}{\rho g} = -\frac{1+\beta}{\beta}\frac{dH}{H} \ , \tag{12}$$

the integration with β = constant leads to

$$\frac{p}{p_0} = \left(\frac{H}{H_0}\right)^{-1/\beta} \ , \tag{13}$$

and

$$\frac{\rho g}{\rho_0 g_0} = \left(\frac{H}{H_0}\right)^{-(1+\beta)/\beta} \ . \tag{14}$$

The expansion of equations (13) and (14) gives

$$\frac{p}{p_0} = \exp\left\{-\frac{z}{\frac{1}{2}(H+H_0)}\left[1 + \frac{1}{3}\left(\frac{H-H_0}{H+H_0}\right)^2 + \frac{1}{5}\left(\frac{H-H_0}{H+H_0}\right)^4 + \ldots\right]\right\} \tag{15}$$

$$\frac{\rho g}{\rho_0 g_0} = \exp\left\{-\frac{(1+\beta)z}{\frac{1}{2}(H+H_0)}\left[1 + \frac{1}{3}\left(\frac{H-H_0}{H+H_0}\right)^2 + \frac{1}{5}\left(\frac{H-H_0}{H+H_0}\right)^4 + \ldots\right]\right\} \qquad (16)$$

The second term in brackets is less than 0.01 at $z = H_0$ if $\beta \leq 0.42$ and at $z = \frac{1}{2} H_0$ if $\beta \leq 0.84$. Neglecting terms less than 0.01 before unity, we can reduce equation (16) to

$$\frac{\rho g}{\rho_0 g_0} = \exp\left(-\frac{(1+\beta)z}{\frac{1}{2}(H+H_0)}\right) , \qquad (17)$$

which is sufficiently accurate when an analysis is made in a height interval less than one scale height.

With a constant gradient of the scale height, equation (10) leads to

$$\beta_\rho = \frac{\beta}{1+\beta} , \qquad (18)$$

and equation (12) becomes

$$\frac{d\rho g}{\rho g} = -\frac{1}{\beta_\rho}\,\frac{dH_\rho}{H_\rho} . \qquad (19)$$

If the same terms are neglected as were for expression (16), equation (19) becomes after integration,

$$\frac{\rho g}{\rho_0 g_0} = \exp\left(-\frac{z}{\frac{1}{2}(H_\rho + H_{0\rho})}\right) . \qquad (20)$$

Equation (15) must be compared with expressions (1) and (20). Since an analysis of the physical conditions of the heterosphere cannot be made without allowing for the effect of the gradient of the scale height, it is useful to have available a variety of atmospheric models for which computations have been carried out for combinations of the scale-height gradients associated with the variations of temperature and of mean molecular mass.

It will be noticed that the difference between the parameter of density H_ρ with its gradient β_ρ and the local atmospheric scale height H with its gradient β increases with increasing values of β.

2. Method of Determining Atmospheric Models

Inspection of density values at 200 km obtained by calculation reveals that the scale-height gradient below 150 km plays the leading role in determining the density at higher altitudes (Nicolet, 1960). In other words, if boundary conditions are assumed in the neighbourhood of 120 km, the atmospheric density between 200 km and 250 km is fixed by the scale-height gradient between 120 km and 150 km but is not much affected by the values of the scale-height gradient above 150 km. The net result is that the vertical distribution of density at high altitudes depends on the temperature at the level of the thermopause, and the variation of the scale-height gradient above the thermopause is due essentially to the decrease of molecular mass. Thus, the atmospheric conditions are defined by a diffusion distribution and related to the time of conduction (Nicolet, 1961a).

From an analysis using various boundary conditions and scale-height gradients, it appears that the temperature must be considered as the most important parameter in deducing the vertical distribution of atmospheric density. Consequently, the vertical distribution of temperature is related to the conditions of heat conduction, and the heterosphere can be assumed to be in diffusion equilibrium. Average conditions lead, therefore, to consistent atmospheric models in which the temperature and its vertical gradient can be determined when diffusion equilibrium is assumed.

The diurnal variation of the density is represented by a change of the temperature and a variation of its vertical gradient. In the same way, the effects of solar activity can be interpreted by a variation of the ultraviolet radiation that affects the temperature gradient and leads to variations of the temperature of the isothermal layer. In fact, it should be possible to predict how the density must vary during a solar cycle when the boundary conditions are known.

Finally, the magnetic storm effects can also be included since Jacchia (1961) has shown that the atmospheric-drag perturbations during geomagnetic disturbances have a worldwide distribution. The interpretation must be that a general heating occurs, corresponding to an increase of the temperature at all latitudes.

It is certain that atmospheric conditions change in the E layer and involve a variation of temperature that is an important parameter to determine boundary conditions for atmospheric models of the heterosphere. We cannot present here all the possibilities, and average conditions have been adopted in order to lead to a density of the order of 4×10^{-12} gm/cm^3 at 200 km. It must be noticed that for the same gradient of temperature, a variation of $\pm$ 50°K at 120 km leads to a variation of $\pm$ 50 percent of the density at 200 km.

The average conditions adopted here are as follows:

Density	$\rho(120 \text{ km}) = 3.5 \times 10^{-11}$ gm/cm^3
Temperature	$T(120 \text{ km}) = 325°$ K
Concentration	$n(0) = 7.6 \times 10^{10}$ oxygen atoms/cm^3
Concentration	$n(O_2) = 1.2 \times 10^{11}$ oxygen molecules/cm^3
Concentration	$n(N_2) = 5.8 \times 10^{11}$ nitrogen molecules/cm^3
Scale-height	H = 10.37 km

3. Atmospheric Conditions from 150 km to 650 km

The vertical distribution of density between 120 km and 150 km is practically unaffected by the form of the variation with height of the scale-height gradient, and the density in the region of 150 to 160 km is almost a constant for the same boundary conditions at 120 km. The values of density to be expected at 150 km for temperatures varying from 877° K to 642° K are given in Table 1. Such a range of temperatures corresponds to equal intervals of times (t = 0, t = 10) for a cooling by conduction of the whole heterosphere considered as a plane-parallel atmosphere subject to diffusion. The 12 models of Table 1 correspond to the following temperatures at 150 km and their associated gradients between 150 km and 160 km:

No.	0	1	1.5	2	3	4	5	6	7	8	9	10
T(° K)	877	873	863	852	829	803	777	751	726	699	671	642
$\left(\frac{dT}{dz}\right)$ km	18	15	14	13	11	10	9	8	7	6	5	4

In Tables 1 to 10, T refers to temperature in $^{\circ}$K; H, the atmospheric scale height in km; β, the gradient of H for the height interval indicated in the table; H_ρ, the density parameter deduced from formula (10); ρ, the density in gm/cm^3 with (-12) for 10^{-12}; p, the pressure in mm Hg with (-6) for 10^{-6}; M, the mean molecular mass with the mass of atomic oxygen M = 16; n, the total concentration in cm^{-3} with (+10) for (10^{10}).

The essential character of the data of Table 1 is that the parameters H_ρ and M are almost constant, while the atmospheric scale height and its gradient vary. The density is almost constant; $(2.5 \pm 0.1) \times 10^{-12}$ gm/cm^3 for temperatures higher than 700°K. Below 700°K, boundary conditions at 120 km are affected.

Since $H_\rho = (20 \pm 1)$ km for the whole range of temperatures, it is clear that density data deduced from satellite air drag may lead to wrong conclusions about the atmospheric structure. For example, a constant scale height is sometimes deduced from an analysis of satellite data even though there is in fact a strong gradient of the atmospheric scale height. When an association was made between the apparent scale height and the temperature, the wrong conclusion was reached that the atmosphere was almost isothermal.

Consequently, Table 1 reveals that the variation of the atmospheric scale height and its gradient can be very important, while other parameters, and particularly the density parameter H_ρ, show no practical variation. Such a variation of the atmospheric scale height must lead to the variation of all physical parameters at higher altitudes.

At 200 km (see Table 2), the gradient of the atmospheric scale height is about 50 percent of its value at 150 km; even for a range of 500° K in the temperature, the density remains practically constant; $\rho = (4.1 \pm 0.1) \times 10^{-13}$ gm/cm^3 for 1050° K $\leq$ T $\leq$ 1550° K. This shows again how important are the boundary conditions that are chosen in the E layer; what is needed is a very small gradient to reduce the 200 km density by an appreciable percentage. However, the variation is more apparent in the pressure, which decreases with decreasing temperature.

Between 250 km and 650 km, the gradient of the atmospheric scale height is generally between $\beta = 0.2$ and 0.1, as can be seen from an inspection of the figures in Tables 3 to 8. Since the gradient is relatively small, the difference between the atmospheric scale height H and the density parameter H_ρ becomes less important, i.e., 20 percent to 10 percent. Nevertheless, the effect of small values of β between 0.1 and 0.2 cannot be neglected since it corresponds to the decrease of the molecular mass in the isothermal layer.

Inspection of figures of physical parameters from 200 km to 650 km shows how their amplitude increases with altitude. For example, at 400 km (see Table 6), the density varies by a factor of 10, and the pressure by a factor of 20, and the mean molecular mass decreases from M = 20.6 to M = 16.6 when the temperature range is between 2100° K and 900° K, corresponding to a variation of H from 97 km to 52 km. Such a general result shows that an arbitrary choice of the mean molecular mass cannot be made as it was for the COSPAR International Reference Atmosphere (1961). It is unwise to attempt to specify atmospheric conditions with an arbitrary molecular mass since it may lead to inconsistent information relevant to the thermal or diffusive equilibrium of the upper atmosphere. Wrong conclusions indicating a decrease of temperature between 400 km and 500 km, such as obtained by Lundback (1961), reveal that the analysis of observational data is not correct since the atmosphere at these altitudes is at least isothermal. It should also be borne in mind that diffusion must adapt the molecular weight mg to the temperature conditions prevailing in the isothermal region, and there is no reason, therefore, to expect some sharp decrease of molecular mass at a particular altitude.

When the molecular mass is more than 14, the gas is presumed to consist essentially of nitrogen and oxygen, and it should be remembered that molecular nitrogen behaves almost in the same way, both for mixing and for diffusion conditions. Its mass M = 28 does not differ very much from the mean molecular

mass of the air, M = 29. Thus, the vertical distribution of molecular nitrogen is closely related to the vertical distribution of temperature in the homosphere and heterosphere. Its concentration at 400 km varies according to temperature conditions defined by Table 6 from 2×10^8 molecules/cm^3 to 5×10^6 molecules/cm^3, i.e., a factor of the order of 40 when its concentration at 150 km remains constant, namely 4×10^{10} molecules/cm^3. Such a large variation affects the mean molecular mass since the corresponding variation in density is the order of a factor of 10.

4. Presence of Helium

It should be noticed from the figures of Tables 7 and 8 that the mean molecular mass becomes less than M = 16. This is due to the introduction of helium. Diffusion leads to an important concentration of helium atoms at the upper levels (Nicolet, 1961b). Physical conditions such as that represented by the already analysed models lead to an almost constant value of n(He) at 500 km. The values of helium concentration do not vary by more than ± 30 percent from an average value for temperatures between 2100° K and 750° K. The absolute value is, however, related to the level of the beginning of diffusion.

Starting from the normal mixing ratio $n(He)/n(N_2)$, the concentration of atomic helium at 105 km is

$$n(He)_{105\ km} = 3.0 \times 10^7 \text{ atoms/cm}^3 \quad . \tag{21}$$

If diffusion begins at that level, the concentration at 500 km is

$$n(He)_{500\ km} = (1.8 \pm 0.5) \times 10^6 \text{ atoms/cm}^3 \quad , \tag{22}$$

when the temperature at 500 km varies from 2133° K (Model No. 0) to 733° K (Model No. 10). If, instead of beginning at 105 km, the diffusion starts at 110 km or 115 km, the concentration given by equation (22) must be decreased by a factor of 2 or 4. A difference of about 5 km of the altitude of the diffusion level corresponds to a difference of a factor of 2 in the concentration of helium.

In the present calculation, we have adopted 105 km as the level where diffusion of helium begins; a correction is easily introduced if diffusion is considered to start at other altitudes.

Table 9, which gives the atmospheric conditions at 650 km, shows how the effect of helium may be important at such altitudes when the temperature is sufficiently low. For example, if $T \leq 1000°$ K corresponding to nighttime conditions at the beginning of 1961, the total density decreases to less than 5×10^{-17} gm/cm^3, while the density of helium reaches about 5×10^{-18} gm/cm^3. The presence of helium leads to a molecular mass less than 12. The effect of helium has also an important consequence. The atmospheric scale-height never decreases below 85 km even if the temperature at 650 km varies by about 1000° K.

The effect of helium is particularly apparent at 900 km, where there is a large variation of the mean molecular mass (see Table 10). The mean molecular mass, which is still of the order of 15 near 2000° K, may reach such a low value as 5 for temperatures less than 1000° K.

Since the perigee heights of the Echo satellite (1960 ι 1) are in the range of 900 to 1600 km, a set of atmospheric data is given in Table 11 for altitudes between 1000 km and 2000 km. The density and concentration of helium are included in Table 11 to allow a comparison with the total density and concentration. A change in the level of diffusion of helium can easily be introduced by an adequate correction.

From an analysis of data on the orbit of Echo I, Zadunaisky, Shapiro and Jones (1961) and Römer (1961) have deduced densities that cannot be explained by an atomic oxygen atmosphere or atomic hydrogen atmosphere, but are in accordance with an effect of helium.

An atomic mass M = 16 would require a temperature too high to fit observational data between 500 km and 700 km. An effect of atomic hydrogen on the mean molecular mass would lead to too high concentrations. The atmospheric-drag perturbations as observed by Jacchia (1961) during geomagnetic disturbances show that the drag of the neutral constituents of the atmosphere has still the most important effect even at altitudes above 1000 km. The figures of Table 11 show how helium can be introduced in the analysis of Zadunaisky, Shapiro and Jones (1961) with scale heights greater than 300 km at 1500 km, and then 150 km at 900 km. The presence of helium is unavoidable above 1000 km.

5. General Tables of ρ, $\rho H^{1/2}$, and H

Table 12 summarizes the vertical distribution of density deduced according to the physical conditions described in the preceding sections and, therefore, the results obtained for the various models already analyzed by their various parameters in Tables 1 to 11. It can be noticed that the levels of constant density increase regularly with increasing temperature. A picture of constant density levels between 500 km and 2000 km is provided in Fig. 1. There is a linear relation between the altitude and the temperature, and the various slopes for curves of constant density show the increasing effect of the temperature when the absolute value of the density decreases. Such relations between temperature and variation of density with height must be related to the diurnal bulge described by Jacchia (1960) and must be also associated with the results of his (1961) accurate analysis of the atmospheric-drag perturbations.

From comparison of the density data of Table 12 with published data on densities deduced from satellite air-drag, a picture of the temperature variation during the years 1958 to 1961 can be provided (Nicolet.1961c). The maximum density obtained in October 1958 corresponds to a temperature between 2000° and 2100° K, while the average value from September 1958 to January 1959 may correspond to a temperature between 1700° and 1800° K. The two density distributions given by Martin and Priester (1961) correspond to about 1750° K and 1150° K. As far as the density distributions given by King-Hele and Walker (1961) are concerned, they represent average conditions showing the variation from 1958 to 1960, namely 1750° K to 1350° K for late-1958 and late-1960 daytime values, and 1050° K to 950° K for late-1959 and late-1960 nighttime values. Even if a systematic error is involved in such a determination, the variation of the temperature shows the general trend of the diurnal variation and the solar activity effect (Nicolet.1961a).

In order to make available a consistent table of parameters more closely associated with data deduced from satellite observations, Table 13 gives the values of $\rho H^{1/2}$ and H from 150 to 2000 km. The value of $H^{1/2}$ is not subject to variation at 150 km for a range of temperatures of about 125° K with defined boundary conditions at 120 km, and a small variation is apparent near 200 km. The maximum variation occurs in the region of 600 to 700 km. At 1000 km (see Fig. 2), the variation for $750 \leq T \leq 1850°$ K corresponds to the variation obtained at 500 km. It should be noticed that $\rho H^{1/2}$ and H do not necessarily vary in the same way, and, therefore, ρ and $\rho H^{1/2}$ may have different variations in the region where different constituents are involved.

References

JACCHIA, L. G.

1960. A variable atmospheric-density model from satellite accelerations. J. Geophys. Res., vol. 65, pp. 2775-2782.

1961. The atmospheric drag of artificial satellites during the October 1960 and November 1960 events. Smithsonian Astrophys. Obs., Special Report No. 62, 13 pp.

KALLMANN-BIJL, H. K., BOYD, R. F. L., LAGOW, H., POLOSKOV, S. M., and PRIESTER, W.

1961. COSPAR International Reference Atmosphere (CIRA, 1961). North-Holland Publishing Co., Amsterdam, 177 pp.

KING-HELE, D. G., and WALKER, D. M. C.

1961. Upper-atmosphere density during the years 1957 to 1961 determined from satellite orbits. Proc. COSPAR Space Symposium, Florence, April 1961, North-Holland Publishing Co., Amsterdam, in press.

LUNDBACK, A.

1961. Atmospheric properties up to 500 km concluded from circular satellite orbits. Publikationer fra Det Danske Meteorologiske Institut, Meddelelser No. 14, pp. 1-17.

MARTIN, H. A., and PRIESTER, W.

1961. Model of atmospheric densities. Proc. COSPAR Space Symposium, Florence, April 1961, North-Holland Publishing Co., Amsterdam, in press.

NICOLET, M.

1954. Dynamic effects in the high atmosphere. Chapter 13, pp. 644-712, in The Earth as a Planet, ed. G. P. Kuiper, The University of Chicago Press, Chicago.

1960. The properties and constitution of the upper atmosphere. Chapter 2, pp. 17-71, in The Physics of the Upper Atmosphere, ed. J. A. Ratcliffe, Academic Press, New York.

1961a. Structure of the thermosphere. Planetary and Space Science, vol. 5, pp. 1-32.

1961b. Helium, an important constituent in the lower exosphere. J. Geophys. Res., vol. 66, pp. 2263-2264.

1961c. Les modèles atmosphériques et l'hélium. Proc. COSPAR Space Symposium, Florence, April 1961, North-Holland Publishing Co., Amsterdam, in press.

RÖMER, M.

1961. Modell der Exosphäre im Höhenbereich 1000-1700 km berechnet aus den Bahnänderungen des Satelliten Echo I. Mitteilung der Universitäts-Sternwarte Bonn Nr. 37, pp. 1-34.

ZADUNAISKY, P. E., SHAPIRO, I. I., and JONES, H. M.

1961. Experimental and theoretical results on the orbit of Echo I. Smithsonian Astrophys. Obs., Special Report No. 61, 22 pp.

Table 1

PHYSICAL PARAMETERS AT 150 KM

No.	T	H	$\beta_{150\text{-}160}$	H_ρ	ρ	p	M	N
0	877	29.8	0.67	20.0	2.41(-12)	5.0(-6)	26.2	5.6(+10)
1	873	29.6	0.56	20.7	2.43	5.0	26.2	5.6
1.5	863	29.3	0.53	20.9	2.45	5.0	26.2	5.6
2	852	28.9	0.48	21.0	2.48	5.0	26.2	5.7
3	829	28.1	0.44	21.0	2.54	5.0	26.1	5.8
4	803	27.3	0.38	21.0	2.59	5.0	26.1	6.0
5	777	26.4	0.35	21.1	2.62	4.9	26.1	6.0
6	751	25.6	0.31	20.8	2.65	4.8	26.1	6.1
7	726	24.7	0.28	20.4	2.61	4.5	26.1	6.0
8	699	23.8	0.28	20.1	2.35	3.9	26.1	5.4
9	671	22.9	0.25	19.8	2.14	3.4	26.0	4.9
10	642	21.2	0.20	19.2	1.97(-12)	3.0(-6)	26.0	4.8(+10)

Table 2

ATMOSPHERIC CONDITIONS AT 200 KM

No.	T	H	$\beta_{200-210}$	H_ρ	ρ	p	M	N
0	1540	56.0	0.32	42.7	4.07(-13)	1.6(-6)	24.8	9.9(+9)
1	1414	51.8	0.27	41.3	4.14	1.5	24.7	1.0(+10)
1.5	1358	49.6	0.25	40.1	4.17	1.4	24.7	1.0
2	1305	47.8	0.23	39.6	4.17	1.4	24.6	1.0
3	1210	44.3	0.20	38.1	4.16	1.3	24.5	1.0
4	1126	41.6	0.18	36.2	4.10	1.2	24.4	1.0(+10)
5	1051	39.0	0.15	34.5	3.98	1.1(-6)	24.3	9.9(+9)
6	985	36.8	0.13	32.0	3.84	9.8(-7)	24.1	9.6
7	925	34.8	0.13	31.3	3.59	8.6	24.0	9.0
8	867	32.8	0.12	30.4	3.03	6.9(-7)	23.8	7.7(+9)

Table 3

ATMOSPHERIC CONDITIONS AT 240 KM

No.	T	H	$\beta_{240-260}$	H_ρ	ρ	p	M	N
0	1791	68.4	0.25	58.8	1.77(-13)	8.3(-7)	23.9	4.5(+9)
1	1613	62.2	0.21	54.2	1.72	7.3	23.7	4.4
1.5	1532	59.3	0.19	52.3	1.70	6.9	23.6	4.3
2	1458	56.7	0.18	49.7	1.66	6.4	23.5	4.2
3	1327	52.0	0.16	49.0	1.58	5.6	23.3	4.1
4	1215	48.2	0.14	44.2	1.47	4.8	23.0	3.8
5	1120	44.9	0.13	41.8	1.35	4.2	22.8	3.6
6	1037	42.1	0.12	39.4	1.23	3.5	22.5	3.3
7	965	39.7	0.11	37.0	1.09(-13)	2.9	22.2	2.9
8	896	37.4	0.10	35.1	8.64(-14)	2.2(-7)	21.9	2.4(+9)

Table 4

ATMOSPHERIC CONDITIONS AT 300 KM

No.	T	H	$\beta_{300-320}$	H_0	ρ	p	M	N
0	1975	81.3	0.18	73.7	6.86(-14)	3.7(-7)	22.6	1.8(+9)
1	1752	73.3	0.16	65.9	6.15	3.0	22.2	1.7
1.5	1650	69.6	0.15	63.3	5.80	2.7	22.0	1.6
2	1556	66.3	0.14	60.6	5.44	2.4	21.8	1.5
3	1393	60.5	0.12	55.5	4.76	1.9	21.4	1.3
4	1261	55.8	0.12	51.7	4.08	1.5	21.0	1.2
5	1150	52.0	0.11	48.8	3.45	1.2(-7)	20.4	1.0(+9)
6	1057	48.7	0.10	46.1	2.89	9.4(-8)	20.2	8.6(+8)
7	978-I(*)	46.0	0.10	43.3	2.35	7.2	19.8	7.2
8	903-I	43.3	0.09	41.0	1.71(-14)	5.0(-8)	19.4	5.3(+8)

(*)Symbol I means the temperature at the thermopause.

Table 5

ATMOSPHERIC CONDITIONS AT 340 KM

No.	T	H	$\beta_{340-360}$	H_ρ	ρ	p	M	N
0	2036	88.0	0.16	80.0	4.00(-14)	2.3(-7)	21.8	1.1(+9)
1	1796	79.4	0.14	72.4	3.40	1.8	21.3	9.6(+8)
1.5	1683	75.3	0.13	68.6	3.13	1.6	21.0	8.9
2	1583	71.6	0.12	65.8	2.86	1.4	20.8	8.3
3	1408	65.2	0.12	61.0	2.36	1.0(-7)	20.3	7.0
4	1271	60.3	0.11	57.2	1.92	7.7(-8)	19.8	5.8
5	1155-I	56.1	0.10	53.6	1.54	5.7	19.4	4.8
6	1059-I	52.6	0.09	49.8	1.23(-14)	4.3	18.9	3.9
7	978-I	49.7	0.08	47.3	9.55(-15)	3.1	18.3	3.1
8	903-I	46.8	0.09	44.8	6.61(-15)	2.0(-8)	18.1	2.2

Table 6

ATMOSPHERIC CONDITIONS AT 400 KM

No.	T	H	$\beta_{400-420}$	H_ρ	ρ	p	M	N
0	2086	96.9	0.14	41.2	1.93(-14)	1.2(-7)	20.6	5.6(+8)
1	1826	87.3	0.13	82.3	1.53	8.7(-8)	20.0	4.6
1.5	1707	82.8	0.12	74.6	1.36	7.3	19.7	4.1
2	1597	78.6	0.11	73.6	1.19	6.1	19.4	3.7
3	1412-I	71.6	0.10	67.7	9.11(-15)	4.2	18.9	2.9
4	1272-I	66.2	0.09	62.7	6.89	3.0	18.4	2.2
5	1155-I	61.5	0.08	59.2	5.16	2.1	18.0	1.7
6	1059-I	57.6	0.07	55.4	3.86	1.4(-8)	17.6	1.3(+8)
7	978-I	54.2	0.08	52.6	2.81	9.9(-9)	17.3	9.8(+7)
8	903-I	52.1	0.09	50.4	1.82(-15)	6.0(-9)	16.6	6.4(+7)

Table 7

ATMOSPHERIC CONDITIONS AT 520 KM

No.	T	H	$\beta_{520-540}$	H_ρ	ρ	p	M	N
0	2123	113.4	0.13	104.0	5.45(-15)	3.9(-8)	18.6	1.8(+8)
1	1837-I	101.6	0.12	95.2	3.85	2.5	17.9	1.3
1.5	1711-I	96.4	0.11	90.9	3.19	1.9	17.6	1.1(+8)
2	1598-I	91.6	0.10	86.5	2.62	1.5(-8)	17.3	9.1(+7)
3	1412-I	83.6	0.09	79.4	1.75	9.2(-9)	16.8	6.3
4	1272-I	77.6	0.08	74.1	1.17(-15)	5.7	16.3	4.3
5	1155-I	72.3	0.09	68.6	7.76(-16)	3.5	15.8	3.0
6	1059-I	68.1	0.10	64.2	5.15	2.2	15.4	2.0
7	978-I	65.0	0.11	60.6	3.35	1.4(-9)	14.9	1.4(+7)
8	903-I	63.6	0.15	58.0	1.92(-16)	7.7(-10)	14.1	8.2(+6)

Table 8

ATMOSPHERIC CONDITIONS AT 560 KM

No.	T	H	$\beta_{560-580}$	H_ρ	ρ	p	M	N
0	2128	118.3	0.12	104.2	3.72(-15)	2.7(-8)	18.0	1.2(+8)
1	1837-I	105.9	0.11	100.2	2.54	1.7	17.4	8.8(+7)
1.5	1711-I	100.4	0.10	95.2	2.06	1.3(-8)	17.1	7.3
2	1598-I	95.4	0.10	90.1	1.66	9.8(-9)	16.8	5.9
3	1412-I	87.1	0.09	83.3	1.06(-15)	5.7	16.3	3.9
4	1272-I	80.9	0.10	76.9	6.85(-16)	3.4	15.8	2.6
5	1155-I	75.8	0.10	70.9	4.36	2.0	15.3	1.7
6	1059-I	72.0	0.12	66.7	2.78	1.2(-9)	14.8	1.1(+7)
7	978-I	69.7	0.16	63.5	1.74(-16)	7.6(-10)	14.1	7.4(+6)
8	903-I	70.2	0.22	60.4	9.65(-17)	4.2(-10)	12.9	4.5(+6)

Table 9

ATMOSPHERIC CONDITIONS AT 650 KM

No.	T	H	$\beta_{650-700}$	H_ρ	ρ	p	M	N
0	2131-I	128.8	0.10	124.2	1.66(-15)	1.3(-8)	17.1	5.9(+7)
1	1837-I	114.8	0.10	109.9	1.07(-15)	7.4(-9)	16.5	3.9
1.5	1711-I	109.0	0.10	104.8	8.25(-16)	5.4	16.2	3.1
2	1598-I	103.8	0.10	99.3	6.32	4.0	15.9	2.4
3	1412-I	95.5	0.11	90.6	3.70	2.1	15.2	1.5(+7)
4	1272-I	90.1	0.12	84.3	2.19	1.2(-9)	14.6	9.1(+6)
5	1155-I	86.8	0.19	78.2	1.28(-16)	6.7(-10)	13.7	5.6
6	1059-I	86.0	0.26	74.5	7.55(-17)	3.9	12.7	3.6
7	978-I	88.3	0.36	72.6	4.42	2.4	11.4	2.3
8	903-I	97.6	0.70	74.9	2.36	1.4(-10)	9.5	1.5(+6)

Table 10

ATMOSPHERIC CONDITIONS AT 900 KM

No.	T	H	$\beta_{900-1000}$	H_ρ	ρ	p	M	N
0	2133-I	156.5	0.14	147.6	2.52(-16)	2.2(-9)	15.1	1.0(+7)
1	1837-I	144.2	0.20	133.0	1.29	1.0(-9)	14.1	5.5(+6)
1.5	1711-I	140.8	0.24	126.9	8.86(-17)	7.0(-10)	13.4	4.0
2	1598-I	140.1	0.30	122.5	6.06	4.8	12.6	2.9
3	1412-I	145.3	0.44	118.6	2.88	2.4	10.7	1.6
4	1272-I	159.6	0.58	122.8	1.47(-17)	1.3(-10)	8.8	1.0(+6)
5	1155-I	180.6	0.61	135.0	7.93(-18)	8.1(-11)	7.1	6.8(+5)
6	1059-I	201.2	0.53	154.8	4.73	5.4	5.8	4.9
7	978-I	216.6	0.39	179.2	3.11	3.8	5.0	3.8
8	903-I	224.9	0.23	205.3	2.18(-18)	2.8(-11)	4.4	3.0(+5)

Table 11

ATMOSPHERIC DATA BETWEEN 1000 KM AND 2000 KM

No.	T	z	H	ρ Total	ρ(Helium)	p	M	N Total	N(He)
0	2133	1000	171	1.28(-16)	6.2(-18)	1.2(-9)	14.2	5.4(+6)	9.3(+5)
		1250	232	2.82(-17)	4.1(-18)	3.4(-10)	11.2	1.5(+6)	6.2(+5)
		1500	352	8.20(-18)	2.8(-18)	1.4(-10)	7.9	6.3(+5)	4.3(+5)
		2000	666	1.79(-18)	1.4(-18)	5.1(-11)	4.2	2.3(+5)	2.1(+5)
1	1837	1000	164	6.08(-17)	5.3(-18)	5.5(-10)	12.7	2.9(+6)	8.0(+5)
		1250	257	1.19(-17)	3.4(-18)	1.6(-10)	8.7	8.3(+5)	5.0(+5)
		1500	412	3.68(-18)	2.2(-18)	7.3(-11)	5.8	3.8(+5)	3.3(+5)
		2000	642	1.05(-18)	9.9(-19)	2.9(-11)	4.2	1.5(+5)	1.5(+5)
1.5	1711	1000	165	4.03(-17)	4.8(-18)	3.6(-10)	11.8	2.0(+6)	7.3(+5)
		1250	278	7.73(-18)	2.9(-18)	1.1(-10)	7.5	6.2(+5)	4.4(+5)
		1500	434	2.59(-18)	1.9(-18)	5.4(-11)	5.1	3.0(+5)	2.8(+5)
		2000	612	8.14(-19)	7.9(-19)	2.1(-11)	4.1	1.2(+5)	1.2(+5)
2	1598	1000	170	2.68(-17)	4.5(-18)	2.5(-10)	10.7	1.5(+6)	6.7(+5)
		1250	303	5.24(-18)	2.6(-18)	8.1(-11)	6.4	4.9(+5)	3.9(+5)
		1500	446	1.94(-18)	1.6(-18)	4.2(-11)	4.6	2.5(+5)	2.4(+5)
		2000	579	6.49(-19)	6.4(-19)	1.6(-11)	4.0	9.7(+4)	9.6(+4)
3	1412	1000	189	1.24(-17)	3.7(-18)	1.3(-10)	8.5	8.8(+5)	5.5(+5)
		1250	339	2.79(-18)	2.0(-18)	4.8(-11)	5.1	3.3(+5)	3.0(+5)
		1500	435	1.22(-18)	1.1(-18)	2.6(-11)	4.2	1.8(+5)	1.7(+5)
		2000	516	4.10(-19)	4.1(-19)	9.0(-12)	4.0	6.1(+4)	6.1(+4)

Table 11 (Cont.)

ATMOSPHERIC DATA BETWEEN 1000 KM AND 2000 KM

No.	T	z	H	ρ Total	ρ(Helium)	p	M	N Total	N(He)
4	1273	1000	216	6.51(-18)	3.0(-18)	7.7(-11)	6.7	5.9(+5)	4.6(+5)
		1250	347	1.79(-18)	1.6(-18)	3.2(-11)	4.4	2.4(+5)	2.3(+5)
		1500	405	8.48(-19)	8.2(-19)	1.6(-11)	4.1	1.2(+5)	1.2(+5)
		2000	466	2.64(-19)	2.6(-19)	5.2(-12)	4.0	4.0(+4)	4.0(+5)
5	1155	1000	241	3.78(-18)	2.5(-18)	5.0(-11)	5.4	4.2(+5)	3.7(+5)
		1250	336	1.24(-18)	1.2(-18)	2.1(-11)	4.2	1.8(+5)	1.8(+5)
		1500	371	5.93(-19)	5.9(-19)	1.1(-11)	4.0	8.9(+4)	8.9(+4)
		2000	423	1.67(-19)	1.7(-19)	3.0(-12)	4.0	2.5(+4)	2.5(+4)
6	1059	1000	254	2.48(-18)	2.0(-18)	3.5(-11)	4.7	3.2(+5)	3.0(+5)
		1250	316	9.04(-19)	8.8(-19)	1.5(-11)	4.1	1.3(+5)	1.3(+5)
		1500	342	4.17(-19)	4.2(-19)	6.8(-12)	4.0	2(+4)	6.2(+4)
		2000	387	1.05(-19)	1.1(-19)	1.7(-12)	4.0	1.6(+4)	1.6(+4)
7	978	1000	255	1.78(-18)	1.6(-18)	2.5(-11)	4.4	2.5(+5)	2.4(+5)
		1250	294	6.71(-19)	6.7(-19)	1.0(-11)	4.0	1.0(+5)	1.0(+5)
		1500	316	2.94(-19)	2.9(-19)	4.5(-12)	4.0	4.4(+4)	4.4(+4)
		2000	358	6.65(-20)	6.7(-20)	1.0(-12)	4.0	1.0(+4)	1.0(+4)
8	903	1000	247	1.34(-18)	1.3(-18)	1.8(-11)	4.1	1.9(+5)	1.9(+5)
		1250	273	4.99(-19)	5.0(-19)	7.0(-12)	4.0	7.5(+4)	7.5(+4)
		1500	292	2.06(-19)	2.1(-19)	2.9(-12)	4.0	3.1(+4)	3.1(+4)
		2000	330	4.11(-20)	4.1(-20)	5.8(-13)	4.0	6.2(+3)	6.2(+4)

Table 12

COMPUTED ATMOSPHERIC DENSITIES

z (km)	No. 0 T_I 2133° K	1 1837	1.5 1711	2 1598	3 1412	4 1272	5 1155	6 1059	7 978	8 903	9 837	10 773
150	-11.618	-11.614	-11.611	-11.606	-11.595	-11.587	-11.582	-11.577	-11.583	-11.629	-11.690	-11.706
160	-11.836	-11.824	-11.818	-11.813	-11.801	-11.793	-11.788	-11.785	-11.796	-11.845	-11.889	-11.932
170	-12.009	-11.996	-11.987	-11.983	-11.971	-11.967	-11.967	-11.967	-11.979	-12.033	-12.086	-12.134
180	-12.154	-12.139	-12.134	-12.130	-12.123	-12.120	-12.123	-12.128	-12.146	-12.206	-12.205	-12.322
190	-12.280	-12.268	-12.264	-12.261	-12.257	-12.259	-12.266	-12.277	-12.301	-12.367	-12.433	-12.498
200	-12.390	-12.383	-12.380	-12.380	-12.381	-12.387	-12.400	-12.416	-12.445	-12.519	-12.592	-12.666
210	-12.492	-12.488	-12.488	-12.490	-12.495	-12.507	-12.526	-12.548	-12.583	-12.662	-12.745	-12.824
220	-12.583	-12.585	-12.588	-12.592	-12.602	-12.622	-12.644	-12.674	-12.714	-12.801	-12.889	-12.979
240	-12.752	-12.765	-12.770	-12.780	-12.801	-12.833	-12.870	-12.910	-12.963	-13.064	-13.168	-13.274
260	-12.900	-12.925	-12.900	-12.955	-12.987	-13.029	-13.078	-13.131	-13.197	-13.311	-13.430	-13.550
280	-13.036	-13.072	-13.096	-13.113	-13.159	-13.214	-13.275	-13.340	-13.419	-13.545	-13.676	-13.810
300	-13.164	-13.211	-13.237	-13.264	-13.322	-13.389	-13.462	-13.539	-13.629	-13.767	-13.910	-14.057
320	-13.284	-13.343	-13.374	-13.408	-13.479	-13.558	-13.640	-13.728	-13.830	-13.979	-14.133	-14.292
340	-13.298	-13.469	-13.505	-13.544	-13.627	-13.717	-13.813	-13.910	-14.020	-14.180	-14.345	-14.514
360	-13.507	-13.588	-13.631	-13.676	-13.770	-13.873	-13.975	-14.085	-14.203	-14.374	-14.548	-14.728
380	-13.613	-13.703	-13.752	-13.801	-13.907	-14.020	-14.134	-14.252	-14.381	-14.561	-14.745	-14.936

Table 12 (Cont.)

COMPUTED ATMOSPHERIC DENSITIES

z (km)	No. 0 T_I 2133° K	1 1837	1.5 1711	2 1598	3 1412	4 1272	5 1155	6 1059	7 978	8 903	9 837	10 773
400	-13.714	-13.815	-13.867	-13.925	-14.041	-14.162	-14.287	-14.413	-14.551	-14.740	-14.936	-15.138
420	-13.810	-13.921	-13.983	-14.042	-14.169	-14.300	-14.434	-14.570	-14.717	-14.910	-15.111	-15.322
440	-13.907	-14.026	-14.090	-14.157	-14.294	-14.434	-14.578	-14.724	-14.876	-15.079	-15.289	-15.511
460	-14.000	-14.127	-14.196	-14.268	-14.416	-14.564	-14.717	-14.870	-15.034	-15.244	-15.462	-15.695
480	-14.089	-14.266	-14.299	-14.376	-14.533	-14.690	-14.854	-15.016	-15.188	-15.405	-15.635	-15.873
500	-14.178	-14.321	-14.398	-14.480	-14.646	-14.813	-14.983	-15.151	-15.330	-15.552	-15.799	-16.047
520	-14.264	-14.415	-14.496	-14.582	-14.757	-14.932	-15.110	-15.290	-15.475	-15.717	-15.959	-16.215
540	-14.347	-14.506	-14.592	-14.682	-14.867	-15.049	-15.237	-15.423	-15.618	-15.867	-16.118	-16.377
560	-14.430	-14.595	-14.686	-14.780	-14.975	-15.164	-15.361	-15.556	-15.760	-16.016	-16.270	-16.532
580	-14.513	-14.682	-14.777	-14.876	-15.079	-15.277	-15.483	-15.686	-15.896	-16.159	-16.418	-16.678
600	-14.592	-14.765	-14.867	-14.971	-15.182	-15.388	-15.602	-15.813	-16.032	-16.299	-16.559	-16.815
650	-14.780	-14.971	-15.084	-15.199	-15.432	-15.660	-15.893	-16.122	-16.355	-16.627	-16.879	-17.113
700	-14.955	-15.168	-15.291	-15.418	-15.672	-15.917	-16.170	-16.413	-16.654	-16.917	-17.148	-17.347
750	-15.126	-15.358	-15.492	-15.629	-15.903	-16.166	-16.433	-16.684	-16.921	-17.165	-17.363	-17.401
800	-15.289	-15.541	-15.684	-15.833	-16.126	-16.403	-16.678	-16.928	-17.154	-17.367	-17.532	-17.674
850	-15.446	-15.719	-15.873	-16.029	-16.338	-16.625	-16.900	-17.143	-17.348	-17.529	-17.670	-17.796
900	-15.599	-15.889	-16.053	-16.218	-16.541	-16.833	-17.101	-17.325	-17.507	-17.662	-17.788	-17.910

Table 12 (Cont.)

COMPUTED ATMOSPHERIC DENSITIES

z (km)	No. 0 T_I 2133° K	1 1837	1.5 1711	2 1598	3 1412	4 1272	5 1155	6 1059	7 978	8 903	9 837	10 773
1000	-15.893	-16.216	-16.395	-16.572	-16.907	-17.186	-17.423	-17.606	-17.750	-17.873	-17.991	-18.119
1250	-16.550	-16.925	-17.112	-17.281	-17.554	-17.747	-17.889	-18.044	-18.173	-18.302	-18.441	-18.600
1500	-17.086	-17.434	-17.587	-17.712	-17.914	-18.072	-18.227	-18.380	-18.532	-18.686	-18.854	-19.048
2000	-17.747	-17.979	-18.089	-18.188	-18.387	-18.578	-18.777	-18.979	-19.177	-19.386	-19.609	-19.867

Table 13

LOG $\rho H^{1/2}$ AND H

z (km)	No. 0 T_I 2133° K	1 1837	1.5 1711	2 1598	3 1412	4 1272	5 1155	6 1059	7 978	8 943	9 837	10 773
150	-8.38	-8.38	-8.38	-8.38	-8.38	-8.37	-8.37	-8.38	-8.39	-8.44	-8.49	-8.54
	29.8	29.6	29.3	28.9	28.1	27.3	26.4	25.6	24.7	23.8	22.9	21.3
160	-8.55	-8.55	-8.55	-8.55	-8.55	-8.55	-8.55	-8.55	-8.57	-8.64	-8.70	-8.74
	36.5	35.2	34.6	33.8	32.5	31.1	29.9	28.7	27.5	26.3	25.1	23.9
170	-8.70	-8.70	-8.70	-8.70	-8.70	-8.70	-8.70	-8.72	-8.74	-8.80	-8.89	-8.92
	42.4	40.1	39.1	38.1	36.2	34.4	32.7	31.2	29.8	28.4	26.9	25.5
180	-8.82	-8.82	-8.82	-8.82	-8.82	-8.82	-8.85	-8.85	-8.89	-8.96	-9.04	-9.11
	47.4	44.4	43.0	41.7	39.3	37.1	35.1	33.3	31.7	30.1	28.4	26.8
190	-8.92	-8.92	-8.92	-8.92	-8.46	-8.46	-9.00	-9.00	-9.04	-9.12	-9.19	-9.28
	52.0	48.2	46.5	44.9	42.0	39.5	37.2	35.2	33.3	31.5	29.7	28.0
200	-9.02	-9.03	-9.03	-9.04	-9.06	-9.08	-9.10	-9.13	-9.17	-9.26	-9.35	-9.43
	56.0	51.6	49.6	47.8	44.5	41.6	39.0	36.8	34.8	32.8	30.9	29.1
210	-9.10	-9.12	-9.13	-9.14	-9.16	-9.19	-9.22	-9.26	-9.30	-9.40	-9.49	-9.59
	59.6	54.6	52.4	50.3	46.6	43.4	40.7	38.3	36.1	34.0	32.1	30.2
220	-9.19	-9.21	-9.22	-9.23	-9.26	-9.29	-9.34	-9.38	-9.43	-9.52	-9.64	-9.74
	62.8	57.3	54.9	52.6	48.6	45.2	42.2	39.6	37.4	35.2	33.2	31.2
240	-9.34	-9.37	-9.39	-9.41	-9.44	-9.49	-9.54	-9.60	-9.66	-9.77	-9.89	-10.01
	68.4	62.1	59.3	56.7	52.0	48.2	44.9	42.1	39.7	37.4	35.2	33.2
260	-9.47	-9.51	-9.54	-9.57	-9.62	-9.68	-9.74	-9.80	-9.89	-10.01	-10.14	-10.28
	73.3	66.3	63.1	60.2	55.1	50.9	47.4	44.4	41.9	39.4	37.3	35.2
280	-9.59	-9.66	-9.68	-9.72	-9.77	-9.85	-9.92	-10.00	-10.10	-10.24	-10.38	-10.52
	77.5	70.0	66.5	63.4	57.9	53.4	49.7	46.6	44.0	41.4	39.2	37.0

Table 13 (Cont.)

LOG $\rho H^{1/2}$ AND H

z (km)	No. 0 T_I 2133° K	1 1837	1.5 1711	2 1598	3 1412	4 1272	5 1155	6 1059	7 978	8 943	9 837	10 773
300	-9.70	-9.77	-9.82	-9.85	-9.92	-10.02	-10.10	-10.19	-10.30	-10.44	-10.60	-10.77
	81.3	73.3	69.6	66.3	60.5	55.8	52.0	48.7	46.0	43.3	41.1	38.8
320	-9.82	-9.92	-9.96	-10.00	-10.08	-10.17	-10.28	-10.38	-10.49	-10.66	-10.82	-11.00
	84.8	76.4	72.6	69.0	62.9	58.1	54.1	50.7	47.9	45.2	42.8	40.4
340	-9.92	-10.02	-10.07	-10.12	-10.22	-10.33	-10.44	-10.55	-10.68	-10.85	-11.02	-11.21
	88.0	79.4	75.3	71.6	65.2	60.3	56.1	52.6	49.7	46.8	44.4	42.0
360	-10.03	-10.13	-10.19	-10.24	-10.36	-10.47	-10.60	-10.72	-10.85	-11.03	-11.22	-11.41
	91.1	82.1	77.9	74.0	67.5	62.4	58.0	54.4	51.3	48.8	46.0	43.8
380	-10.12	-10.24	-10.30	-10.36	-10.48	-10.62	-10.74	-10.89	-11.02	-11.21	-11.41	-11.62
	94.1	84.8	80.4	76.4	69.6	64.4	59.8	56.1	52.8	50.6	48.0	45.7
400	-10.22	-10.35	-10.42	-10.48	-10.62	-10.74	-10.89	-11.04	-11.19	-11.39	-11.60	-11.82
	96.9	87.3	82.8	78.6	71.6	66.2	61.5	57.6	54.2	52.1	49.5	47.4
420	-10.31	-10.44	-10.52	-10.59	-10.74	-10.89	-11.04	-11.19	-11.35	-11.55	-11.74	-12.00
	99.6	89.7	85.1	80.0	73.5	68.0	63.1	59.0	55.7	53.9	51.5	49.3
440	-10.40	-10.55	-10.62	-10.70	-10.85	-11.01	-11.17	-11.34	-11.49	-11.70	-11.92	-12.16
	102	92.0	87.2	82.8	75.3	69.6	64.5	60.7	57.4	55.4	53.4	51.5
460	-10.49	-10.64	-10.72	-10.80	-10.96	-11.14	-11.31	-11.48	-11.66	-11.85	-12.09	-12.33
	105	94.3	89.3	84.7	77.3	71.1	66.6	62.5	59.2	57.1	55.2	54.0
480	-10.57	-10.74	-10.82	-10.92	-11.09	-11.26	-11.44	-11.62	-11.80	-12.02	-12.25	-12.49
	107	96.8	91.7	87.1	79.6	73.4	68.2	64.5	61.1	59.0	57.5	57.2
500	-10.66	-10.82	-10.92	-11.00	-11.19	-11.38	-11.55	-11.74	-11.92	-12.17	-12.41	-12.66
	111	99.5	94.4	89.7	81.8	75.9	70.6	66.4	63.2	61.1	60.4	61.3

Table 13 (Cont.)

LOG $\rho H^{1/2}$ AND H

z (km)	No. 0 T_I 2133° K	1 1837	1.5 1711	2 1598	3 1412	4 1272	5 1155	6 1059	7 978	8 943	9 837	10 773
520	-10.74	-10.92	-11.00	-11.10	-11.30	-11.49	-11.68	-11.89	-12.07	-12.32	-12.55	-12.80
	113	102	96.4	91.6	83.6	77.6	72.3	68.1	65.0	63.6	63.9	66.3
540	-10.82	-11.00	-11.10	-11.19	-11.40	-11.60	-11.80	-12.00	-12.21	-12.46	-12.70	-12.96
	116	104	98.4	93.6	85.4	79.2	74.0	70.0	67.2	66.7	68.2	72.5
560	-10.89	-11.08	-11.19	-11.29	-11.51	-11.72	-11.92	-12.18	-12.34	-12.59	-12.85	-13.08
	118	106	100	95.4	87.1	80.9	75.8	72.0	69.7	70.2	73.4	80.0
580	-10.96	-11.16	-11.28	-11.39	-11.60	-11.82	-12.04	-12.25	-12.47	-12.72	-12.96	-13.21
	121	108	102	97.3	88.8	82.7	77.8	74.3	72.8	74.6	79.8	88.8
600	-11.05	-11.24	-11.36	-11.47	-11.70	-11.92	-12.15	-12.37	-12.59	-12.85	-13.09	-13.32
	123	110	104	99.2	90.6	84.6	80.0	77.1	76.2	79.9	87.3	99.1
650	-11.22	-11.44	-11.57	-11.70	-11.96	-12.18	-12.42	-12.66	-12.89	-13.13	-13.36	-13.55
	129	115	109	104	95.5	90.1	86.8	86.0	88.3	97.6	111	128
700	-11.40	-11.64	-11.77	-11.89	-12.17	-12.42	-12.68	-12.92	-13.14	-13.38	-13.57	-13.74
	134	120	114	109	101	97.3	96.3	98.9	106	122	141	156
750	-11.55	-11.80	-11.96	-12.10	-12.39	-12.66	-12.92	-13.15	-13.37	-13.57	-13.74	-13.92
	139	125	119	114	108	107	110	117	130	152	170	179
800	-11.70	-12.00	-12.14	-12.29	-12.59	-12.85	-13.12	-13.36	-13.55	-13.74	-13.89	-14.03
	145	131	125	121	118	120	128	142	159	181	193	194
850	-11.85	-12.15	-12.31	-12.47	-12.80	-13.06	-13.31	-13.52	-13.70	-13.89	-14.01	-14.14
	150	137	132	130	130	137	152	171	189	206	210	203

Table 13 (Cont.)

LOG $\rho H^{1/2}$ AND H

z (km)	No. 0	1	1.5	2	3	4	5	6	7	8	9	10
	T_I 2133° K	1837	1711	1598	1412	1272	1155	1059	978	943	837	773
900	-12.00	-12.31	-12.48	-12.64	-12.96	-13.23	-13.47	-13.68	-13.85	-14.00	-14.11	-14.25
	156	144	141	140	145	160	181	201	217	225	221	210
1000	-12.28	-12.62	-12.80	-12.96	-13.27	-13.52	-13.72	-13.92	-14.05	-14.18	-14.31	-14.44
	171	164	165	170	189	216	241	254	255	248	234	218
1250	-12.85	-13.22	-13.39	-13.54	-13.80	-14.00	-14.14	-14.29	-14.44	-14.59	-14.74	-14.92
	232	257	278	303	339	347	336	316	294	273	254	234
1500	-13.31	-13.62	-13.77	-13.89	-14.09	-14.27	-14.44	-14.62	-14.80	-14.96	-15.14	-15.35
	352	412	435	446	435	405	371	342	316	292	271	250
2000	-13.85	-13.08	-14.19	-14.31	-14.54	-14.74	-14.96	-15.18	-15.40	-15.62	-15.85	-16.14
	666	642	611	579	516	466	423	388	358	330	306	283

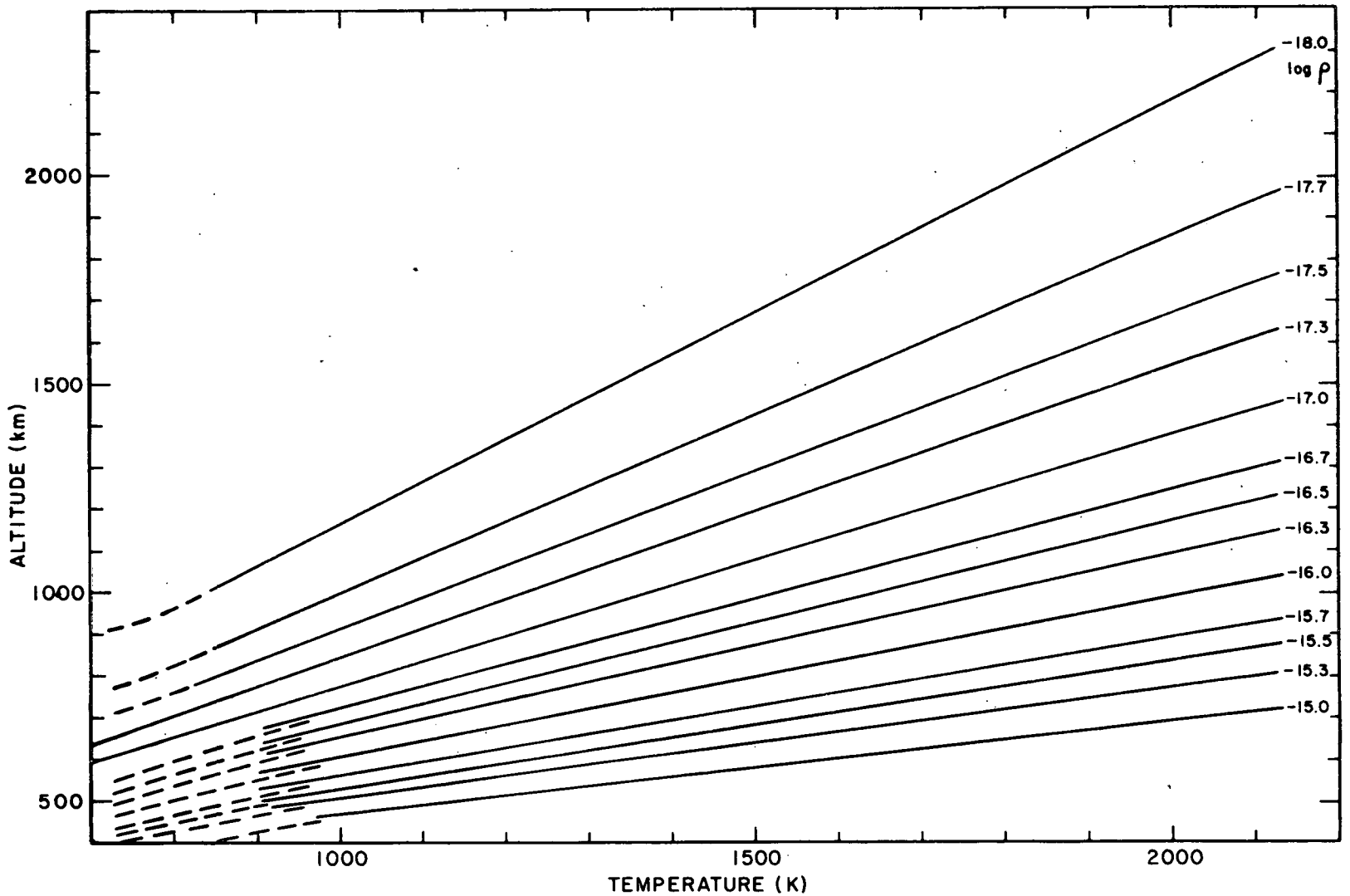

Figure 1. --Altitudes of surfaces of equal density as a function of the temperature.

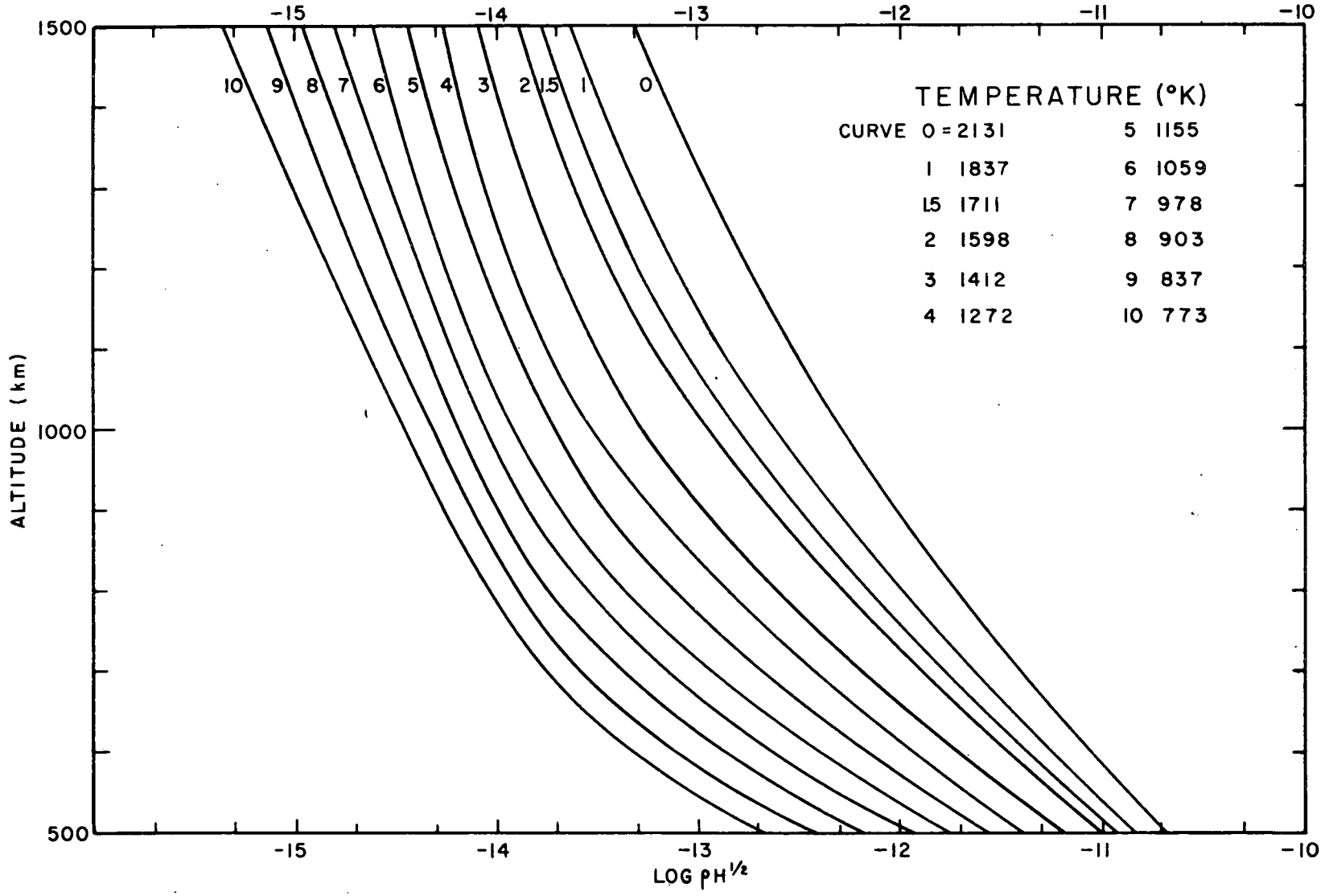

Figure 2. --Vertical distribution of log $\rho H^{1/2}$ as a function of temperature.